Applied Energy 362 (2024) 122940

Contents lists available at ScienceDirect

Applied Energy

journal homepage: www.elsevier.com/locate/apenergy

A bioaugmentation strategy to recover methane production under sulfate-stressed conditions: Highlights on targeted sulfate-reducing bacteria and DIET-related species

Ginevra Giangeri [a], Panagiotis Tsapekos [a], Maria Gaspari [b], Parisa Ghofrani-Isfahani [a], Laura Treu [c], Panagiotis Kougias [b], Stefano Campanaro [c,*,1], Irini Angelidaki [a,*,1]

[a] Department of Chemical and Biochemical Engineering, Technical University of Denmark, DK-2800 Kgs. Lyngby, Denmark
[b] Soil and Water Resources Institute, Hellenic Agricultural Organization Dimitra, Thermi, Thessaloniki 57001, Greece
[c] Department of Biology, University of Padova, Via U. Bassi 58/b, 35121 Padua, Italy

HIGHLIGHTS

- A novel combined approach with magnetite and *Methanosarcina barkeri* to improve AD systems.
- Methane yield enhanced while effectively reducing TVFA and H2S production.
- qPCR monitoring for early microbial shift detection to ensure AD with prompt response.
- Challenges with long-term persistence of bioaugmentation in complex microbial ecosystems.

GRAPHICAL ABSTRACT

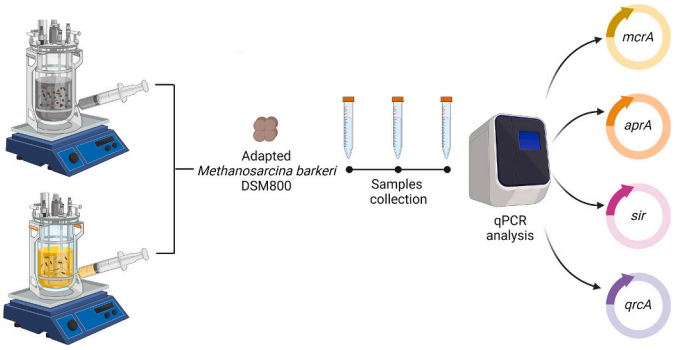

ARTICLE INFO

Keywords:
Anaerobic digestion
Methanosarcina barkeri
Bioaugmentation
Quantitative polymerase chain reaction
Direct interspecies electron transfer

ABSTRACT

Bioaugmentation has been recognized as a key strategy to improve the anaerobic digestion efficiency in organic waste treatment. *Methanosarcina barkeri* possesses direct interspecies electron transfer capability, a characteristic that allows it to outcompete other unwanted species such as sulfate-reducing bacteria. This study investigated the effects of bioaugmentation with *Methanosarcina barkeri* DSM800 on two continuous-stirred tank reactors fed with a sulfate-rich feedstock. One of the two reactors was supplemented with magnetite to facilitate direct interspecies electron transfer. Time series quantitative polymerase chain reactions were performed to evaluate the absolute abundance of crucial species, including the augmented *Methanosarcina*. Results showed increased and stabilized methane production of 22% and 21% in the reactor amended with magnetite and in the control reactor, respectively. Moreover, volatile fatty acids were almost completely consumed in the magnetite-supplemented reactor. The quantitative polymerase chain reaction was used to analyze the abundance of targeted species in response to bioaugmentation. Specifically, *Methanosarcina barkeri* was not retained in either reactor after one hydraulic retention time. Direct interspecies electron transfer-associated microorganisms showed opposite trends

* Corresponding authors.
E-mail addresses: stefano.campanaro@unipd.it (S. Campanaro), iria@kt.dtu.dk (I. Angelidaki).
[1] Equal contribution.

https://doi.org/10.1016/j.apenergy.2024.122940
Received 22 November 2023; Received in revised form 23 February 2024; Accepted 27 February 2024
Available online 11 March 2024

in the two reactors, highlighting the different interactions with *Methanosarcina barkeri* in the presence and absence of magnetite. Sulfate-reducing bacteria following the dissimilatory sulfate reduction pathway exhibited an opposite behavior in the reactor amended with magnetite, in contrast to those employing the assimilatory sulfate reduction pathway. Overall, the study demonstrated that bioaugmentation with exogenous archaea can considerably alter the microbial community, but the introduced species is not able to establish itself in a stable microbiome. In addition, the strategy could be further tested to control H_2S production in real-world waste treatment scenarios. Quantitative polymerase chain reaction proved to be a useful tool for monitoring changes in the absolute abundance of microorganisms in bioreactors, implementing effective monitoring and control strategies to improve overall system performance.

1. Introduction

Anaerobic digestion (AD) is an efficient process for organic waste treatment to produce renewable energy, which relies upon the interdependent metabolic activity of a complex microbial community [1]. The four AD steps – hydrolysis, acidogenesis, acetogenesis, and methanogenesis – are promoted by distinct functional microbial guilds, including hydrolytic and fermentative bacteria, acetogenic and syntrophic bacteria, and methanogenic archaea [2]. However, the methanogenesis step is negatively impacted by the accumulation of some compounds including ammonia, and hydrogen sulfide. More specifically, sulfate reduction can result in the accumulation of hydrogen sulfide, which can considerably inhibit the archaeal metabolic activity [3–5]. Acetotrophic and hydrogenotrophic sulfate reduction are thermodynamically more favorable than acetoclastic and hydrogenotrophic methanogenesis under indirect interspecies electron transfer (IHT) [6,7]:

Hydrogenotrophic sulfate reduction:	
$4H_2 + SO_4^{2-} + H^+ \rightarrow 4H_2O + HS^-$	($\Delta G'_o = -192.0$ kJ/mol)
Hydrogenotrophic methanogenesis:	
$4H_2 + HCO_3^- + H+ \rightarrow 3H_2O + CH_4$	($\Delta G'_o = -175.4$ kJ/mol)
Acetoclastic methanogenesis:	
$CH_3COO^- + H_2O \rightarrow CH_4 + HCO_3^-$	($\Delta G'_o = -31.0$ kJ/mol)
Acetotrophic sulfate reduction:	
$CH_3COO^- + SO_4^{2-} \rightarrow HS^- + 2HCO_3^-$	($\Delta G'_o = -47.6$ kJ/mol)

This thermodynamic property results in the outcompetition of methanogens by sulfate-reducing bacteria (SRB), when sulfate accumulates in the system. In recent years, different strategies have been suggested to overcome issues related to AD process instability, including the use of conductive materials (CMs) and bioaugmentation [8–12]. CMs provide an alternative route for interspecies energy exchange, known as direct interspecies electron transfer (DIET), which bypasses the need to rely solely on H_2 and formate [13,14]. For this reason, CMs have been proposed as a solution to favor methanogens and alleviate the competition with SRBs under sulfate-rich conditions [12,15,16]. On the other hand, several bioaugmentation strategies have been developed to mitigate methanogenesis inhibition using both methanogenic archaea and bacteria [17–19]. In principle, the insufficient performance of a bioreactor might be attributed to an unbalanced microbiome composition, including, for example, a limited amount or activity of specific microorganisms possessing a pivotal metabolic pathway needed to perform a required biochemical process. Bioaugmentation in lab-scale systems has been evaluated using mixed microbial consortia and pure archaeal cultures to increase their abundance and, therefore, favor methanogenesis [8,11,18–21]. In most cases, the augmented microorganisms were acclimatized prior to their addition into the system [20]. Moreover, the enrichment of specific microbes in AD systems has been investigated using microorganisms other than methanogens. For example, photosynthetic bacteria have been applied to recover from VFA inhibition [22], and syntrophic acetate and propionate oxidizing consortia were used to recover from ammonia inhibition [11]. Combining bioaugmentation with a DIET-performing methanogen, such as *Methanosarcina barkeri*, in conjunction with CMs to stabilize the AD process operated at high sulfate levels represents a pioneering approach This strategy harnesses the synergistic effects of bioaugmentation and CMs to enhance the competitiveness of methanogens against SRBs. Notably, this innovative strategy offers a promising avenue for improving and stabilizing methane production efficiency and overcoming the inhibitory effects of high sulfate levels. Although the effectiveness of bioaugmentation strategies in improving the stability of AD processes has been demonstrated, there is a lack of standardized methods for evaluating the establishment and performance of the inoculated microorganisms [18,21]. Additionally, the need to evaluate how bioaugmentation alters the composition of the microbial community poses a remarkable challenge. Due to these limitations, the bioaugmentation strategy is still considered a procedure with unpredictable outcomes [23]. One of the main issues is that the introduced microbial strain(s) might be unable to grow and become active in the bioreactor. This inability could be attributed to several factors such as predation or competition with the indigenous microbiota, the presence of bacteriophages, or the failure to acclimate to the prevailing environmental conditions [25]. Under such dynamic and fluctuating circumstances, characterized by conditions like pH or organic load variations, starvation periods, and suboptimal temperatures, the introduced microorganisms are unlikely to colonize or exhibit population dominance [26–28]. Addressing this issue would facilitate the reliable and reproducible application of bioaugmentation techniques, thereby promoting their widespread adoption and potential for impact. Among the different techniques that could be used for monitoring the bioaugmented microorganism, quantitative polymerase chain reaction (qPCR) might constitute a fast and reliable approach. Compared to other molecular biology techniques such as Next-Generation Sequencing (NGS), Fluorescence In Situ Hybridization (FISH), and older techniques like Denaturing Gradient Gel Electrophoresis (DGGE), qPCR offers several advantages. It is a technique that stands out for its sensitivity, specificity, and real-time monitoring capabilities, allowing for accurate quantification of target nucleic acids in a time-efficient manner compared to DGGE which has limited resolution and may not capture all genetic variants. Moreover, qPCR is cost-effective compared to NGS which, on the other hand, provides more comprehensive genetic information, and to FISH which, in contrast, offers spatial information and single-cell analysis.

In this work, two continuous-stirred tank reactors (CSTRs) fed with a sulfate-rich feedstock - of which one supplemented with magnetite as CM and the other used as a control - [24], were subjected to bioaugmentation with a pure strain of *M. barkeri* DSM800. The CSTRs were monitored for 45 days from the onset of bioaugmentation, and in this period samples were collected at three separate time intervals for further analyses. qPCR was performed to monitor the evolution of five microbial species: *M. barkeri* DSM800, two SRBs, and two bacterial species with potential for DIET performance. This study provides insight into the impact of bioaugmentation with *M. barkeri* DSM800 on microbial populations in CSTRs treated with magnetite under sulfate-rich conditions and the effect of magnetite on DIET. Finally, the potential of qPCR in monitoring the bioaugmented archaeon and its impact on some key microorganisms was explored.

2. Materials and methods

2.1. Lab-scale reactors monitoring

The inoculum, biopulp, and reactors setup used in this study are described in [24]. Briefly, the two lab-scale CSTRs (R-ctrl and R-mag), each of 2.3 and 1.8 L total and working volume respectively, were operated under mesophilic conditions (37 ± 1 °C). The hydraulic retention time (HRT) was set to 23 days by a daily supply of 70 mL diluted biopulp, leading to a constant organic loading rate (OLR) of 2.30 gVS/L-reactor.day. The experimental period was divided into four phases, the reactors were started and when the steady-state was reached – phase 1 - P1 (days 0–44) - sodium sulfate (Na_2SO_4 suitable for HPLC, LiChropur™, 99.0–101.0%, Sigma -Aldrich) was added as a single pulse in (phase 2 - P2 - days 45–68) to reach 0.6 g SO_4^{2-}/L in both CSTRs. Subsequently, the CSTRs were fed with Na_2SO_4-rich biopulp to maintain the sulfate content at the desired value. In phase 3 (P3, days 69–109) the Na_2SO_4 level was increased to 1.2 g SO_4^{2-}/L in both CSTRs and feedstocks. In phase 4 (P4, days 110–197), magnetite (Iron(II, III) oxide powder, <5 μm, 95%, Sigma-Aldrich) was added progressively only in R-mag to reach a final concentration of 10 g/L. In this work, the last phase P5 (days 198–237), involved the implementation of a bioaugmentation strategy, as explained below.

2.2. Bioaugmentation strategy

A pure culture of *Methanosarcina barkeri* DSM800 was obtained from DSMZ-German Collection of Microorganisms and Cell Cultures GmbH, Germany. Before the bioaugmentation experiment, the pure culture was cultivated in three phases, in batch bottles (250 and 100 mL total and working volume, respectively). In the first step, the *Methanosarcina* medium (no. 120) provided by DSMZ for *Methanosarcina* cultivation was used. The pure culture was sub-inoculated when the microorganism reached the late exponential phase. The volatile suspended solids (VSS) calculated at this point of the microbial growth reported a concentration value of 46 mg/L. The subsequent transfer was performed in an adaptation medium composed of 80% *Methanosarcina* medium (no. 120) and 20% filter-sterilized digestate obtained from the two CSTRs; this step was performed to adapt *M. barkeri* to the composition of the medium in the reactors. The last transfer was performed using a medium composition of 60% *Methanosarcina* medium (no. 120) and 40% filter-sterilized digestate from the CSTRs. The bioaugmentation was performed with an inoculum corresponding to 20% of the reactors working volume and was carried out in three days during which the pumps were disconnected to avoid the washout of the microorganism. At operational days 198, 199, and 200, 120 mL of the adapted cultures in the late exponential phase were centrifuged for 10 min at 4500 rpm under N_2 gas headspace. A 60 mL volume of the supernatant was discarded and the pellet was resuspended in the remaining 60 mL of the supernatant to up-concentrate the inoculum. The 60 mL volume obtained for both adapted cultures was anaerobically collected with a syringe and transferred into the reactors.

2.3. DNA extraction and cells count

Samples of 15 mL were collected before (day 197), immediately after (day 201), and after one HRT from the bioaugmentation (day 223) for DNA extraction. Genomic DNA was isolated and purified using the DNeasy PowerSoil® (QIAGEN 181 GmbH, Hilden, Germany) following the manufacturer's protocols with minor modifications [9]. Genomic DNA quantity was determined using Qubit fluorometer (Life Technologies, Carlsbad, CA).

To estimate the number of cells present in 15 mL, the samples were mixed with 35 mL of phosphate buffer saline 1× (PBS, 137 mM NaCl, 2.7 mM KCl, 10 mM Na_2HPO_4, 1.8 mM KH_2PO_4) containing 0.15% Tween-80 and kept into a shaking incubator (37 ± 1 °C, 115 rpm, KS 4000 i control, IKA®-Werke GmbH & Co. KG, Germany). This step favored the release of microorganisms growing attached to the large particles [29]. Samples were centrifuged at 500 rpm for 10 min, the supernatant was collected and centrifuged at 1000 rpm for 10 min to pellet down and remove large particulate. The collected supernatant was filtered in three steps: at the beginning using filters having 40 μm pore size, subsequently with filters having 10 μm pore size, and finally, with filters having 5 μm pore size to remove smaller particles (5–40 μm) and recover the cells. In the final step, samples were centrifuged at 7000 rpm to collect the cells, while the supernatant containing volatile solids (VS) was discarded. The cells were resuspended in 15 mL PBS 1× and volatile suspended solids (VSS) were measured [30].

2.4. Segmented microscopy imaging

A technology developed by ParticleTech Aps in Farum, Denmark was used for non-invasive analysis of particles and cells using microscopy imaging. The solution included a microscope imaging unit, a sampling unit, and software with segmentation and feature-extraction algorithms. The device is based on FluidScopeTM technology to scan particles and cells in a variable volume of liquid (from designed chips to multi-well plates) [31]. This technology captures a number of 6.25◦ tilted images that are then stacked to analyze the particles and cells. The equipment can be used for at-line, on-line, and off-line applications. In this study, off-line analysis was conducted, in which the sample was manually delivered into a microtiter plate. The samples were diluted 1:200 before the analysis. The plate was then placed in the microscope imaging unit to capture images that were later processed using the associated software. The images were combined to obtain a best-focus microscopy image that ensured focus on the floating particles and cells. The best-focus microscopy images were obtained immediately after (day 201), and after one HRT (day 223) after the bioaugmentation to assess the enrichment of *M. barkeri* DSM800 in the CSTRs.

2.5. Primers design, validation, and construction of the calibration curve for qPCR data

From the previous sequencing data analysis [24], four metagenome-assembled genomes (MAGs) were selected for qPCR analysis, together with the bioaugmented *M. barkeri* DSM800. Specifically, the genes targeted were: the gene encoding the adenylylsulfate reductase (*aprA*, EC 1.8.99.2, dissimilatory sulfate reduction pathway) of Peptococcaceae sp. DTU26, a key regulatory point in sulfate assimilation and reduction; the gene codifying the sulfite reductase (*sir*, EC 1.8.7.1, assimilatory sulfate reduction pathway) of *Prevotella* sp. DTU28, which catalyzes the reduction of sulfite to H_2S and water; the gene encoding menaquinone reductase, multi-heme cytochrome *c* subunit (*qrcA gene*) of Myxococcota sp. DTU66, and the gene encoding a type IV pilin protein (*pilA*) of Clostridiaceae sp. DTU102, which indicates its exoelectrogenic capacity [24]. The *pilA* gene was translated using BLASTx and subsequently aligned to the known *pilA* genes of *Geobacter sulfurreducens* and *Geobacter metallireducens* using Clustal Omega [32,33]. Primer-BLAST was used to design the primers [34]. Two primer pairs were selected per each target and were validated through PCR amplification (Eppendorf Thermocycler PCR MasterCycler 5332 Personal, Eppendorf, HA Germany) and gel electrophoresis (Consort E132 Mini Electrophoresis Power Supply, Consort, Turnhout, Belgium) to assess the performance. The primers were prioritized according to the results of the PCR in terms of target specificity to avoid the formation of non-specific target amplification, primer-dimer formation to exclude the self-complementarity in the primers, reducing PCR efficiency, and amplicon size to ensure proper qPCR amplification in all reactions. The PCR reaction was carried out with Taq PCR Core Kit (QIAGEN GmbH, Hilden, Germany) using the manufacturer's protocol for 25 cycles. The agarose gel (1% agarose) was prepared using 50 mL of Tris Acetate-EDTA Buffer 1× (MERCK, Rahway, NJ, USA), 0.5 g agarose (agarose BioReagent, for molecular biology, low EEO, Sigma Aldrich, USA), and 5 μL of SYBR® Green I nucleic acid gel

stain 10,000× (Merck, Rahway, NJ, USA). The gel electrophoresis was run for 20 min at 5 V/cm. The sequences and characteristics of the selected primers are reported in Table 1.

The amplicons obtained from the PCR amplification were purified using the QUIAquick PCR Purification Kit (QIAGEN GmbH, Hilden, Germany) and quantified with Qubit fluorometer (Life Technologies, Carlsbad, CA, US). The purified amplicons were then used as standards to build the calibration curve and, for each, five dilutions were prepared (from 2′000 to 20′000'000 copies, with 10× multiplier). The qPCR reaction was carried out with the PerfeCTa SYBR® Green FastMix (QuantaBio, Beverly, MA, US) following the manufacturer's protocol, using AriaMx Real-time PCR System (Agilent Technologies Inc., Santa Clara, CA, US). All samples and standards were prepared in duplicate and analyzed with the "Replicates: Treated Collectively" function active.

2.6. Absolute quantification

The absolute quantification was performed by integrating two previously reported methods [35,36]. The procedure was made simpler by using the same threshold cycle for both standards and samples. The one-point calibration (OPC) method was selected to correct for quantitative PCR efficiency variations for microbial community samples [35]:

$$N_{0\ sample} = N_{0\ standard} \times \frac{E_{standard}^{C_T}}{E_{sample}^{C_T}}$$

The method accounts for template-related variability of the efficiency (E) by correcting for differences in E between the sample and standard. OPC involves the use of a standard that contains a specific and predetermined quantity of template copies known as $N_{0\ standard}$. Each standard point reaction mixture contained from $2{\cdot}10^3$ to $2{\cdot}10^7$ copies. $N_{0\ standard}$ was calculated as interpolation of the power regression of the number of copies (as defined above) over the number of cycles (obtained from the analysis). As $E_{standard}$, the values calculated from the AriaMx software (v2.0) at the threshold cycle (C_T) defined for both standards and samples were used. The amplification plot method was used to define the E_{sample} [36]. In this method, a fluorescence midpoint (M) is defined as:

$$M = R_{noise} \times \sqrt{\frac{R_{max}}{R_{noise}}}$$

where R_{max} is the fluorescence maximum for each plot and R_{noise} is the standard deviation of the first ten cycles that reflect the fluorescence background prior to amplification. Then, E_{sample} is calculated as the slope defined through the linear regression of three to four points around M (with $R^2 > 0.99$). All the calculations are reported in Supplementary file S1.

2.7. Analytical methods

The methods used to measure total solids (TS), volatile solids (VS), and volatile suspended solids (VSS) were performed following the procedure reported by the American Public Health Association (APHA) standard methods guidelines [30]. The composition of the biogas produced was analyzed using gas chromatography (GC-TRACE 1310, Thermo Fisher Scientific, US) equipped with a thermal conductivity detector (TCD) and Thermo (P/N 26004–6030) Column (30 m length, 0.320 mm inner diameter, and film thickness 10 μm) with helium as carrier gas. Total volatile fatty acids (TVFA) concentrations were measured using gas chromatography (Agilent 7890A, Agilent Technologies, US) equipped with a flame ionization detector (FID) and SGE capillary column (30 m length, 0.53 mm inner diameter, film thickness 1.00 μm) with helium as carrier gas. The injection volume was 1 μL, and every sample was analyzed in duplicate to ensure the precision and reproducibility of the measures. The injector temperature was kept at 150 °C and the detector temperature was at 220 °C. The initial temperature of the column oven was held at 45 °C for 3.5 min and then increased to 210 °C at a ramping rate of 15 °C/min, then held for 4 min at 210 °C. The pH trend was monitored using FiveEasy Plus Benchtop FP20 (Mettler Toledo, CH). H_2S accumulation in the headspace of the reactors was measured with a Geotech BIOGAS 5000 portable gas monitor (QED Environmental Systems Ltd., UK). Specifically, 100 mL of biogas were collected from the headspace, diluted with 700 mL of N_2 into a gasbag, and the mixed gasses were passed into the instrument for measurement.

3. Results and discussion

3.1. Bioaugmentation and reactors performance

Magnetite addition resulted in a 10% ± 1% ($p < 0.05$) increase in methane yield in the reactor with magnetite (R-mag), with an average of 332 ± 19 $mLCH_4/gVS$ [24]. The bioaugmentation was performed with *M. barkeri* DSM800 and this process changed the performance of the CSTRs, particularly affecting the methane yield and reducing TVFA accumulation. The effect of *M. barkeri* DSM800 on the methane yield was remarkable and was already evident shortly after the bioaugmentation, with an increased methane yield of nearly 20% in both reactors. The average methane yield values calculated from the day before the bioaugmentation (day 197) to the day after one HRT from the bioaugmentation (day 225) were 399 ± 21 $mLCH_4/gVS$ and 335 ± 30 $mLCH_4/gVS$ in R-mag and R-ctrl, respectively. Notably, the steady-state at days 210–226, established after the addition of *M. barkeri* DSM800, was characterized by a stable methane yield of 407 ± 6 $mLCH_4/gVS$ and 354 ± 2 $mLCH_4/gVS$ for R-mag and R-ctrl, respectively (Fig. 1a, Supplementary file S3). Biochemical results evidenced the possible establishment of *M. barkeri*. In addition, the increase in methane yield could be attributed to the enhanced syntrophic interactions occurring between acetogens and methanogens; this could be due to the fact that magnetite can act as an electron sink facilitating interspecies electron transfer [14,37].

Previous experimental results revealed that magnetite addition resulted in a considerable decline in TVFA levels [24]. However, the introduction of *M. barkeri* DSM800 in R-mag led to a stronger reduction

Table 1
Characteristics of the primers used for qPCR. In the first column, the forward (F) and reverse (R) primer IDs are reported. In the other columns, additional characteristics are reported including the melting temperature (Tm), the GC content (GC%), the self complementarity (Self compl.), and the self 3′-complementarity (Self 3′ compl.).

Primer ID	Sequence (5′ ➔ 3′)	Template strand	Length	Start	Stop	Tm	GC%	Self compl.	Self 3′ compl.	Product length
mcrA_F	GCCGGTGTTGCCTGCT	Plus	16	1285	1300	60.32	68.75	4.00	0.00	95
mcrA_R	CTGCCCCATGCTTCCTTGT	Minus	19	1379	1361	60.30	57.89	4.00	0.00	
aprA_F	GACTACCCGGAAATGGACGA	Plus	20	16	35	59.18	55.00	4.00	0.00	90
aprA_R	GCGCTTTGCGCAGGTC	Minus	16	105	90	59.81	68.75	6.00	0.00	
sir_F	TGACACTGACGGGAAAGTGG	Plus	20	501	520	59.89	55.00	4.00	2.00	
sir_R	TGAGGACAGGTGAGGTAGCA	Minus	20	640	621	59.89	55.00	2.00	0.00	140
qrcA_F	AACAAAAGGAGGGACTCGGC	Plus	20	12	31	60.25	55.00	3.00	2.00	79
qrcA_R	CATGCCTATCAACCCAGCCA	Minus	20	90	71	60.11	55.00	4.00	0.00	

in TVFA, ultimately resulting in a remarkably low accumulation of acetate (~25 mg/L). Magnetite can compensate for the lack of the multiheme cytochrome OmcS by creating an interconnection between electrically conductive cells, favoring *Methanosarcina barkeri* metabolism through direct electron transfer [14]. In contrast, after the bioaugmentation, R-ctrl displayed unstable TVFA levels ranging from 350 to 1500 mg/L, but without showing any coherent decline in concentration (Fig. 1b, Supplementary file S3). This finding is in agreement with a previous study reporting no remarkable effect on TVFA reduction due to the addition of *M. barkeri* DSM800 in sequencing batch reactors (SBR) [38]. Taken together, these results suggested that the combination of magnetite with the bioaugmented methanogen synergistically enhanced the consumption of TVFA, a result that was impossible to achieve with only the addition of the archaea. These findings bear substantial implications for anaerobic digester management due to the adverse effects of elevated TVFA levels, including acidification in cases of low buffering capacity and, finally, reduced biogas production. TVFA accumulation can result in operational challenges, as well as decreased efficiency and profitability. The presence of magnetite enhanced electron transfer dynamics within the microbial community. Magnetite acted as an electron sink, promoting the formation of conductive networks that facilitated DIET between syntrophic partners, including *Methanosarcina barkeri* DSM800 and acetogenic bacteria. The enhanced electron transfer accelerated the rate of acetate conversion to methane, contributing to the observed reduction in TVFA accumulation and the corresponding increase in methane yield. Despite the fluctuation in TVFA accumulation, the pH remained stable in both CSTRs throughout the whole operation, with values ranging from 7.3 to 7.7 (Fig. 1c, Supplementary file S3).

H_2S measurements performed before and after bioaugmentation revealed that magnetite addition to R-mag caused a marked reduction in H_2S levels [24], from an average of 5000 ± 200 ppm to 16 ± 8 ppm. After the bioaugmentation with *M. barkeri* DSM800, the H_2S level in R-mag remained stable at 16 ± 8 ppm, whereas, in R-ctrl, H_2S decreased to 1336 ± 110 ppm (Fig. 1d, Supplementary file S3). Based on the measurements of methane yield, these findings suggest that the presence of *M. barkeri* DSM800 in R-ctrl could displace SRBs through competitive exclusion, despite magnetite was not present. The bioaugmentation

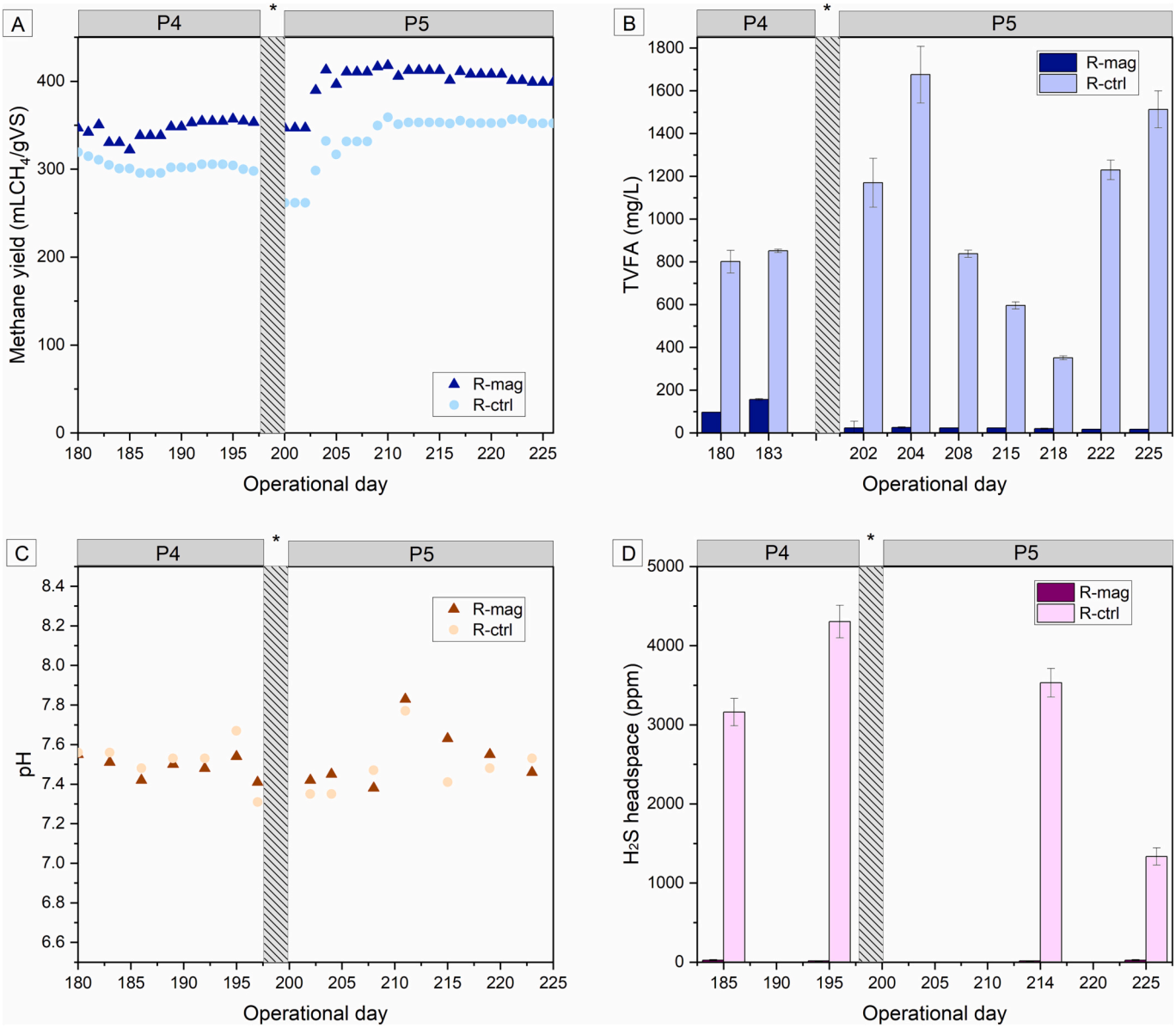

Fig. 1. Overall CSTRs performance before (P4) and after (P5) the bioaugmentation: Methane yield measurements (A), TVFA trend (B), pH drift (C), H_2S concentration (D). The (*) symbol marks the bioaugmentation (performed from day 197 to day 199).

facilitated the methanogen competition with SRB for the same carbon source (i.e. acetate).

3.2. qPCR revealed the washout of *M. barkeri* after one HRT from the bioaugmentation

Segmented microscopy observation of the samples after (Fig. 2 A, B) and one HRT after (Fig. 2 C, D) the bioaugmentation provided a qualitative glimpse of the presence of *M. barkeri* DSM800 (Fig. 2). Images obtained seven days after the bioaugmentation showed the presence of spherical-shaped clusters resembling the classical coccal morphology of *M. barkeri* DSM800. These clusters were clearly distinguishable from the rest of the sample, suggesting a successful bioaugmentation. The morphology of the clusters was consistent with the characteristics reported in previous studies [39,40], suggesting that the augmented *M. barkeri* DSM800 was thriving in the anaerobic conditions of the CSTRs (Fig. 2 A, B). However, coccoidal morphologies were no longer visible after one HRT from the bioaugmentation (Fig. 2 C, D). This finding suggested the potential washout of the augmented microorganism from the systems. To confirm the presence and abundance of *M. barkeri* DSM800 in the reactors, quantitative analysis using qPCR was performed before and after its addition into the reactors, to evaluate the difference in abundance after the bioaugmentation and after one HRT to estimate its potential retention or eventual washout. The results of the qPCR revealed a conspicuous increase in the abundance of the archaea immediately after the bioaugmentation in both reactors (Fig. 5, Table 2). However, at the end of the bioaugmentation, different values were observed in the two reactors, which might be attributed to the presence of magnetite in R-mag. Magnetite could have provided an advantage for the initial establishment of the microbial culture, as previous studies demonstrated the ability of *M. barkeri* to perform DIET. Nonetheless, after one HRT from the bioaugmentation, the results revealed that the abundance of the methanogen drastically decreased in both reactors (Fig. 5, Table 2). The decrease in abundance was almost comparable to the values observed before the bioaugmentation, suggesting that the augmented microorganism was not able to establish a stable population in the system. The inability of the augmented microorganism to establish a stable population may be

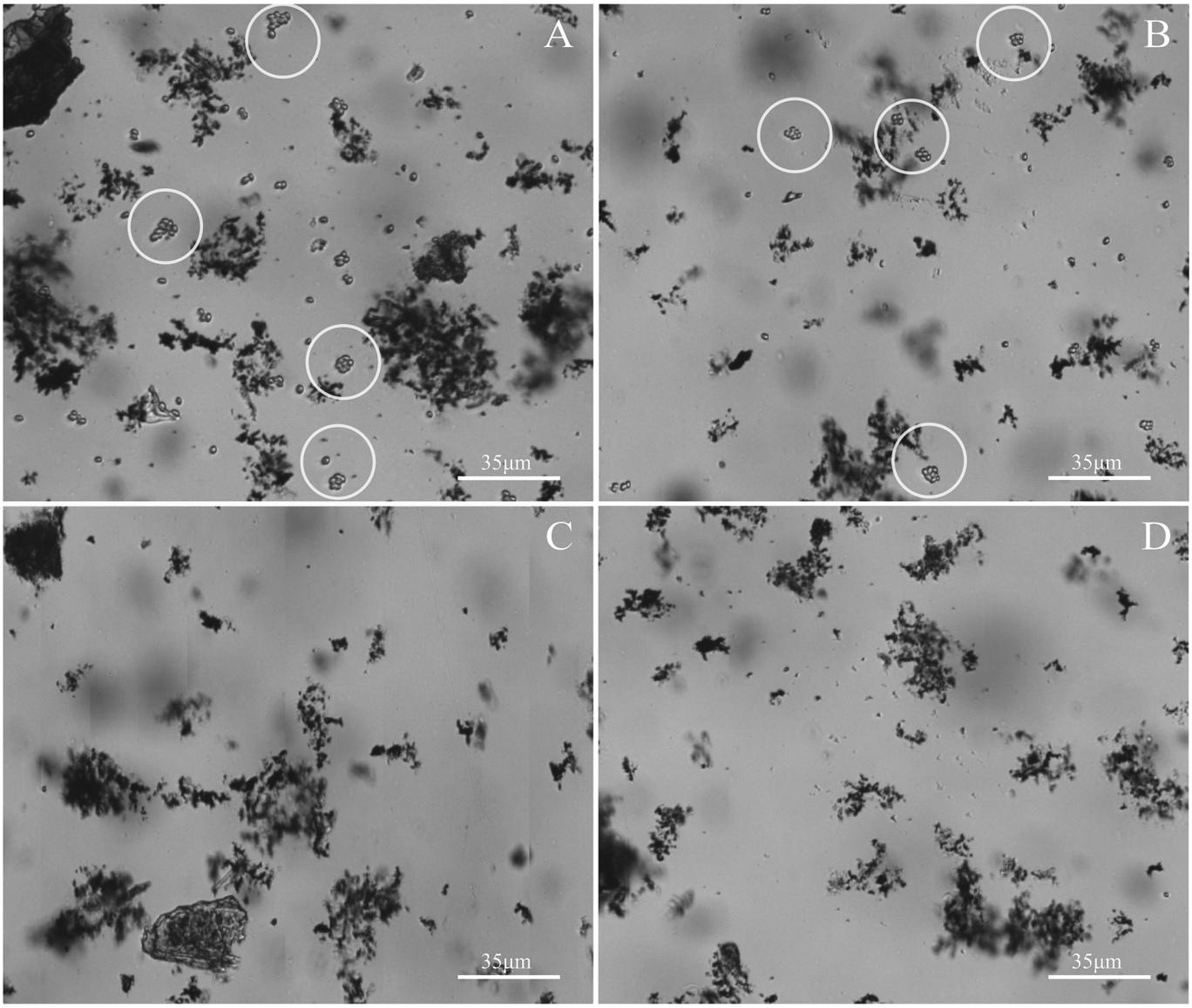

Fig. 2. Segmented imaging microscopy of the collected samples after (A, B) and one HRT after (C, D) the bioaugmentation. The white circles (A, B) highlight the clusters resembling the typical coccal morphology of *M. barkeri*, clearly distinguishable from the rest of the sample. The clusters are no longer visible in the images collected after one HRT from the bioaugmentation.

Table 2
Absolute quantification calculated considering the estimated total number of cells. Operational day (Op. day) 197, 201, and 223 refers to the condition: "before the bioaugmentation" (day 197), "immediately after the bioaugmentation" (day 201), "one HRT after the bioaugmentation" (day 223). All the calculations for baseline correction, efficiency of the sample, absolute quantification, and total number of copies present in the reactors are reported in Supplementary File S2.

Op. day	R-mag				Rctrl			
	aprA	*mcrA*	*sir*	*qrcA*	*aprA*	*mcrA*	*sir*	*qrcA*
197	$2.89 \cdot 10^{7}$	$1.83 \cdot 10^{2}$	$1.03 \cdot 10^{7}$	$1.01 \cdot 10^{7}$	$3.38 \cdot 10^{5}$	$3.00 \cdot 10^{-1}$	$5.80 \cdot 10^{3}$	$1.10 \cdot 10^{8}$
201	$3.98 \cdot 10^{7}$	$1.88 \cdot 10^{5}$	$2.14 \cdot 10^{5}$	$5.30 \cdot 10^{7}$	$2.88 \cdot 10^{4}$	$8.43 \cdot 10^{4}$	$4.10 \cdot 10^{4}$	$1.20 \cdot 10^{8}$
223	$5.06 \cdot 10^{7}$	$2.89 \cdot 10^{3}$	$1.29 \cdot 10^{1}$	$2.38 \cdot 10^{7}$	$1.92 \cdot 10^{3}$	$2.67 \cdot 10^{3}$	$1.84 \cdot 10^{2}$	$2.50 \cdot 10^{8}$

attributed to the microbiome present in both reactors which outcompeted the augmented archaea for resources and niche space. To avoid washout, a potential strategy would be to further adapt the augmented microorganism to the environment present in the bioreactors. Initiating the growth of the microorganism in batch conditions using >40% sterilized digestate may lately facilitate the establishment of the microorganism in the reactors following bioaugmentation. Consequently, the microorganism retention could potentially be enhanced, contributing to the formation of a stable microbiome. Despite the washout of the augmented archaea observed after one HRT, the methane yield increased and remained stable after the inoculation with *M. barkeri* DSM800 in both reactors. These results are in accordance with previous studies reporting a stabilization of methane yield after the bioaugmentation with *M. barkeri* [38,41]. The process of bioaugmentation potentially mitigated the stress induced by competition between methanogens and SRBs, which led to the displacement of SRBs and facilitated the proliferation of methanogens, including *Methanosaeta* spp., that were impeded by substrate competition. Thus, the combination of magnetite and bioaugmentation with *M. barkeri* DSM800 appeared to synergistically enhance the AD process by reducing the adverse effects of SRBs and promoting the proliferation of methanogens. While magnetite can improve the stability of AD systems by promoting the overall microbial metabolism, *M. barkeri* DSM800 can enhance methane production and reduce H_2S concentration by outcompeting SRBs. Eventually, qPCR was a powerful technique for absolute gene copy number quantification, offering high sensitivity, accuracy, and a wide dynamic range, though the limitations included the reliance on standard curves and potential amplification biases. While the precision of the standard curves can be adjusted by the operator experience and precision, amplification biases constitute an issue that should be further mathematically addressed when calculating absolute abundances.

3.3. Effect of *M. barkeri* DSM800 addition on targeted species

The initial MAGs selected for the analysis, their relative abundance, and the targeted gene are reported in Fig. 3. This method was used to investigate the fluctuations in the abundance of specific targeted MAGs. The raw data extracted from the qPCR analysis are reported in Fig. 4. Magnetite is a well-known conductive material, and is expected to stimulate the growth of microorganisms able to exploit DIET in R-mag. Indeed, the two MAGs previously identified as potential DIET performers, are Myxococcota sp. DTU66, which showed the presence of the *qrcA* gene, and Clostridiaceae sp. DTU102, which had a *pilA* gene involved in electron transfer [42–44]. In particular, referring to *pilA* genes, two isoforms are known, a long form involved in bacterial motility and a short form involved in electron transfer [44]. It is worth mentioning that Vargas and colleagues defined the required, despite non-sufficient, conserved aminoacidic sequence to define a pilin as a protein involved in electron transfer [42]. The results of the multialignment confirmed that the motif is conserved in Clostridiaceae sp. DTU102, meaning that it might be potentially involved in DIET. Despite this result, metagenomics revealed that the *pilA* gene identified was not a single-copy gene and was excluded from the qPCR analysis as it would have made it difficult to properly quantify, comparing a multi-copy gene with single-copy genes [45]. Due to this limitation, the investigation was performed only with the *qrcA* gene of Myxococcota sp. DTU66. The quantification of this taxon revealed a similar trend to that of *M. barkeri* DSM800 in R-mag, with an increase in abundance after bioaugmentation, followed by a decrease after one HRT (Fig. 5, Table 2). In contrast, Myxococcota sp. DTU66 revealed a 2-fold increase in R-ctrl after one HRT from the bioaugmentation, suggesting that it was able to thrive in the absence of magnetite and without interacting with the augmented *M. barkeri* DSM800. The particular behavior can be due to the fermentative metabolism of this species (Fig. 5, Table 2) [46]. Thereby, the results suggested that Myxococcota sp. DTU66 possessed the ability to exploit its DIET capabilities in R-ctrl, indicating that magnetite is not required for its growth and survival. This finding emphasizes the importance of investigating the ability of microorganisms to perform DIET in the absence of such materials. Data obtained from the previous study confirmed that most of the genes involved in the assimilatory and dissimilatory sulfate reduction pathways were identified in *Prevotella* sp. DTU28 and Peptococcaceae sp. DTU26, respectively [24].

Fig. 3. Representation of the four targeted MAGs before the bioaugmentation. From left to right: Completeness (Compl.), contamination (Cont.), and relative abundance (RA) of the reconstructed genomes, targeted sequence is highlighted with the initial and final bases targeted by the primers, and gene acronym is reported.

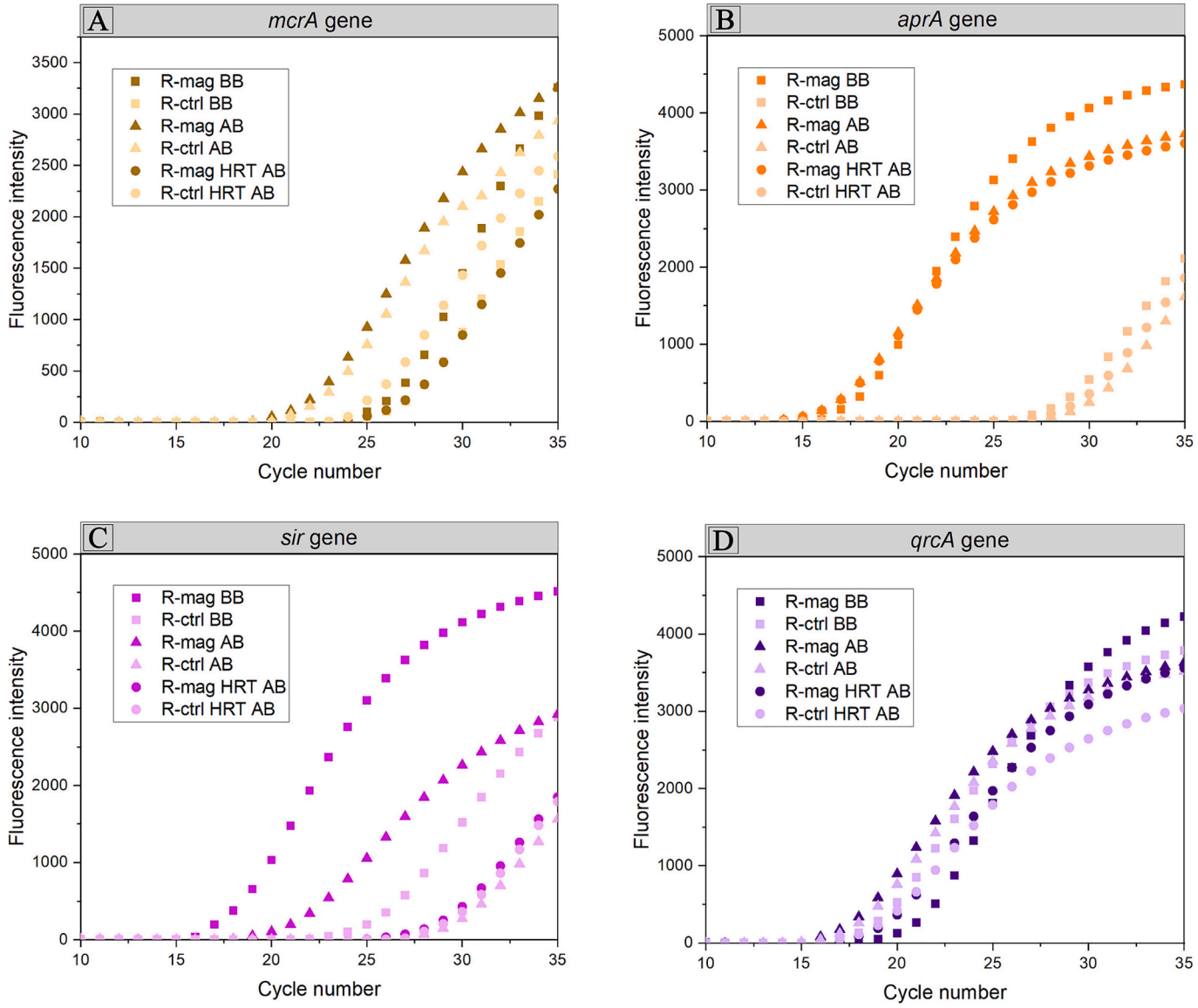

Fig. 4. Amplification plots generated from the qPCR software. The four targeted genes were: the gene encoding the methyl coenzyme M reductase (*mcrA* – A), the adenylylsulfate reductase (*aprA* – B), the sulfite reductase (*sir* – C), and the menaquinone reductase (*qrcA* – D). The qPCR analysis was performed before the bio-augmentation (BB), immediately after the bioaugmentation (AB), and one HRT after the bioaugmentation (HRT AB). Ligh and dark colors refer to control reactor (R-ctrl) and the magnetite-supplemented reactor (R-mag) respectively.

The assimilatory sulfate reduction pathway is used by microorganisms to incorporate sulfate into organic molecules such as cysteine and methionine, and other sulfur-containing compounds.

In contrast, the dissimilatory sulfate reduction pathway is an anaerobic respiratory process producing energy through the sulfate to sulfide reduction process, generating ATP and reducing equivalents such as NADH or hydrogen. The quantification of Peptococcaceae sp. DTU26 showed that this taxon had a 1.5-fold increase in R-mag, while it decreased in R-ctrl (Fig. 5, Table 2). On the contrary, *Prevotella* sp. DTU28 was highly abundant in R-mag before the bioaugmentation, while it sharply decreased in both reactors after the bioaugmentation until the end of the experiment (Fig. 5, Table 2). This result confirms the previous findings which suggested the competition between acetoclastic methanogens and SRBs [24]. In the case of Peptococcaceae sp. DTU26, the presence of cytochrome *c*-encoding genes can potentially provide a competitive advantage to this taxon allowing it to survive and thrive by exploiting DIET and attenuating the competition with the augmented *M. barkeri* DSM800 in R-mag. Besides, in R-ctrl the increased abundance of *M. barkeri* DSM800 after the bioaugmentation may have outcompeted the SRB. Regarding *Prevotella* sp. DTU28, the increased abundance of the methanogen, combined with the incapability of performing DIET, might have constituted the reason for the marked reduction of this taxon in both reactors. Overall, the addition of *Methanosarcina barkeri* DSM800 resulted in the depletion of specific resources such as CO_2 and acetate, leading to notable shifts in microbial community composition within the AD system. This depletion likely influenced the competitive interactions among microbial taxa, driving changes in relative abundance and potentially fostering the emergence of new metabolic pathways. Hence, *M. barkeri* DSM800 not only had an impact on the targeted species but more globally influenced the whole microbial community; qPCR allowed to detect the long-term shift determined by *M. barkeri* even after the washout. Thus, the possibility of retaining the bioaugmented microorganism within the reactors could help predict the microbial community shift and obtain reproducible results.

4. Conclusions and future perspectives

Overall, the results of this study provide valuable insights into the

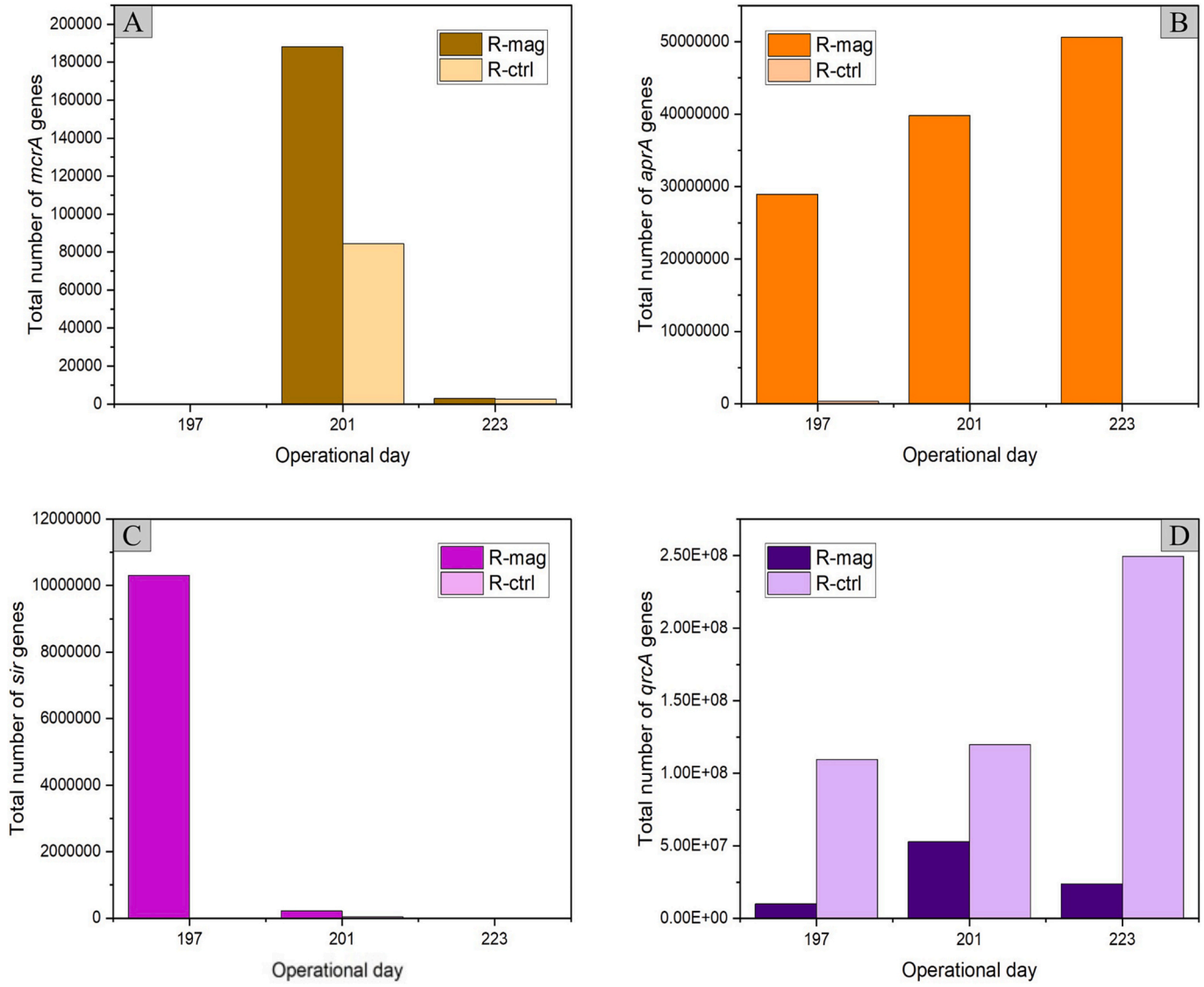

Fig. 5. Absolute quantification calculated from the estimated number of cells. The image shows the absolute quantification of the gene encoding the methyl co-enzyme M reductase (*mcrA* – A), the adenylylsulfate reductase (*aprA* – B), the sulfite reductase (*sir* – C), and the menaquinone reductase (*qrcA* – D). The qPCR analysis was performed before the bioaugmentation (day 197), immediately after the bioaugmentation (day 201), and one HRT after the bioaugmentation (day 223). Light and dark colors highlight the control reactor (R-ctrl) and the magnetite reactor (R-mag), respectively. Standard deviations are not reported since replicates are treated with the "replicates treated collectively" options active.

potential of combining different strategies to enhance the performance of AD processes. The findings suggested that magnetite addition and bioaugmentation with acetoclastic archaea such as *M. barkeri* DSM800 can enhance methane yield while effectively reducing TVFA and H_2S production. This process represents a sustainable solution for treating organic waste while concurrently producing biogas. Moreover, the study highlights the need for further research to optimize the implementation of these strategies in full-scale AD systems. Additionally, the rapid and reliable monitoring capabilities of qPCR demonstrated in this study present a promising avenue for early detection of microbial shifts following bioaugmentation, enabling timely interventions to maintain AD processes. Moreover, the study demonstrated the meaningful impact of *M. barkeri* DSM800 on the targeted species and the overall microbial community, as well as the long-term shift in the microbiome composition provoked by its addition, despite its eventual washout. Furthermore, the results underscore the challenges associated with the long-term persistence of augmented microorganisms in complex microbial ecosystems. Further research is needed to identify the factors impacting the stability and persistence of augmented microorganisms and to develop strategies to enhance their retention and effectiveness in such systems.

Supplementary data to this article can be found online at https://doi.org/10.1016/j.apenergy.2024.122940.

CRediT authorship contribution statement

Ginevra Giangeri: Data curation, Formal analysis, Investigation, Methodology, Validation, Visualization, Writing – original draft. **Panagiotis Tsapekos:** Conceptualization, Methodology, Resources, Validation. **Maria Gaspari:** Investigation, Methodology. **Parisa Ghofrani-Isfahani:** Conceptualization. **Laura Treu:** Data curation, Methodology. **Panagiotis Kougias:** Methodology, Supervision. **Stefano Campanaro:** Data curation, Methodology, Supervision, Writing – review & editing. **Irini Angelidaki:** Conceptualization, Project administration, Resources, Supervision, Writing – review & editing.

Declaration of competing interest

The authors declare that they have no known competing financial interests or personal relationships that could have appeared to influence the work reported in this paper.

Data availability

The important data produced in this worked are shared in Supplementary File S1 and Supplementary File S2. Other data can be made available upon request.

Acknowledgments

This work was supported by Novo Nordisk Foundation under the project framework DIET-Syntrophy "Direct interspecies electron transfer-based syntrophic metabolism between sulfate-reducing bacteria and methanogens via conductive materials" (grant reference no. NNF21OC0071392) and by the European Research Council under the project framework ANAEROB "The ANAEROBic Treasure Trunk" (ERC advanced grant no. 101098064). We thank Assoc. Prof. Seyed Soheil Mansouri and Dr. Nima Nazemzadeh for the support provided with the segmented microscopy analysis.

References

[1] Angelidaki I, Ellegaard L, Ahring BK. Applications of the anaerobic digestion process. In: Ahring BK, Ahring BK, Angelidaki I, Dolfing J, Euegaard L, Gavala HN, et al., editors. Biomethanation II [Internet]. Berlin: Heidelberg: Springer Berlin Heidelberg; 2003. https://doi.org/10.1007/3-540-45838-7_1 [cited 2023 Mar 2]. p. 1–33. (Scheper T, Babel W, Blanch HW, Endo I, Enfors SO, Fiechter A, et al., editors. Advances in Biochemical Engineering/Biotechnology; vol. 82). Available from:.

[2] Campanaro S, Treu L, Kougias PG, Luo G, Angelidaki I. Metagenomic binning reveals the functional roles of core abundant microorganisms in twelve full-scale biogas plants. Water Res 2018 Sep;140:123–34.

[3] Ruiz-Sánchez J, Campanaro S, Guivernau M, Fernández B, Prenafeta-Boldú FX. Effect of ammonia on the active microbiome and metagenome from stable full-scale digesters. Bioresour Technol 2018 Feb;250:513–22.

[4] Treu L, Tsapekos P, Peprah M, Campanaro S, Giacomini A, Corich V, et al. Microbial profiling during anaerobic digestion of cheese whey in reactors operated at different conditions. Bioresour Technol 2019 Mar;275:375–85.

[5] Vu HP, Nguyen LN, Wang Q, Ngo HH, Liu Q, Zhang X, et al. Hydrogen sulphide management in anaerobic digestion: a critical review on input control, process regulation, and post-treatment. Bioresour Technol 2022 Feb;346:126634.

[6] Jung H, Kim D, Choi H, Lee C. A review of technologies for in-situ sulfide control in anaerobic digestion. Renew Sustain Energy Rev 2022 Apr;157:112068.

[7] Paulo LM, Stams AJM, Sousa DZ. Methanogens, sulphate and heavy metals: a complex system. Rev Environ Sci Biotechnol 2015 Dec;14(4):537–53.

[8] Tsapekos P, Kougias PG, Vasileiou SA, Treu L, Campanaro S, Lyberatos G, et al. Bioaugmentation with hydrolytic microbes to improve the anaerobic biodegradability of lignocellulosic agricultural residues. Bioresour Technol 2017 Jun;234:350–9.

[9] Zhu X, Treu L, Kougias PG, Campanaro S, Angelidaki I. Converting mesophilic upflow sludge blanket (UASB) reactors to thermophilic by applying axenic methanogenic culture bioaugmentation. Chem Eng J 2018 Jan;332:508–16.

[10] Sun M, Shi Z, Zhang C, Zhang Y, Zhang S, Luo G. Novel long-chain fatty acid (LCFA)-degrading Bacteria and pathways in anaerobic digestion promoted by Hydrochar as revealed by genome-centric metatranscriptomics analysis. Cann I, editor. Appl Environ Microbiol 2022 Aug 23;88(16). e01042-22.

[11] Li MT, Rao L, Wang L, Gou M, Sun ZY, Xia ZY, et al. Bioaugmentation with syntrophic volatile fatty acids-oxidizing consortia to alleviate the ammonia inhibition in continuously anaerobic digestion of municipal sludge. Chemosphere. 2022 Feb;288:132389.

[12] Yin Q, Gu M, Wu G. Inhibition mitigation of methanogenesis processes by conductive materials: a critical review. Bioresour Technol 2020 Dec;317:123977.

[13] Lovley DR. Syntrophy Goes electric: direct interspecies Electron transfer. Annu Rev Microbiol 2017 Sep 8;71(1):643–64.

[14] Liu F, Rotaru AE, Shrestha PM, Malvankar NS, Nevin KP, Lovley DR. Magnetite compensates for the lack of a pilin-associated *c* -type cytochrome in extracellular electron exchange: magnetite compensates for the lack of OmcS. Environ Microbiol 2015 Mar;17(3):648–55.

[15] Hu J, Zeng C, Liu G, Lu Y, Zhang R, Luo H. Enhanced sulfate reduction accompanied with electrically-conductive pili production in graphene oxide modified biocathodes. Bioresour Technol 2019 Jun;282:425–32.

[16] Zhang Y, Zhang L, Yu N, Guo B, Liu Y. Enhancing the resistance to H2S toxicity during anaerobic digestion of low-strength wastewater through granular activated carbon (GAC) addition. J Hazard Mater 2022 May;430:128473.

[17] Costa JC, Barbosa SG, Sousa DZ. Effects of pre-treatment and bioaugmentation strategies on the anaerobic digestion of chicken feathers. Bioresour Technol 2012 Sep;120:114–9.

[18] Cirne DG, Björnsson L, Alves M, Mattiasson B. Effects of bioaugmentation by an anaerobic lipolytic bacterium on anaerobic digestion of lipid-rich waste. J Chem Technol Biotechnol 2006 Nov;81(11):1745–52.

[19] Westerholm M, Levén L, Schnürer A. Bioaugmentation of syntrophic acetate-oxidizing culture in biogas reactors exposed to increasing levels of Ammonia. Appl Environ Microbiol 2012 Nov;78(21):7619–25.

[20] Yan M, Treu L, Campanaro S, Tian H, Zhu X, Khoshnevisan B, et al. Effect of ammonia on anaerobic digestion of municipal solid waste: inhibitory performance, bioaugmentation and microbiome functional reconstruction. Chem Eng J 2020 Dec;401:126159.

[21] Cavaleiro AJ, Sousa DZ, Alves MM. Methane production from oleate: assessing the bioaugmentation potential of *Syntrophomonas zehnderi*. Water Res 2010 Sep;44 (17):4940–7.

[22] Zhao W, Jeanne Huang J, Hua B, Huang Z, Droste RL, Chen L, et al. A new strategy to recover from volatile fatty acid inhibition in anaerobic digestion by photosynthetic bacteria. Bioresour Technol 2020 Sep;311:123501.

[23] Herrero M, Stuckey DC. Bioaugmentation and its application in wastewater treatment: a review. Chemosphere. 2015 Dec;140:119–28.

[24] Giangeri G, et al. Magnetite alters the metabolic interaction between methanogens and sulfate-reducing Bacteria. Environ Sci Technol Oct. 2023. https://doi.org/10.1021/acs.est.3c05948. p. acs.est.3c05948.

[25] Yan M, Wang C, Li Y, Tian H, Sun Y. Effect of bioaugmentation on psychrotrophic anaerobic digestion: bioreactor performance, microbial community, and cellular metabolic response. Chem Eng J 2023 Jan;455:140173.

[26] He Z, Zhang K, Wang H, Lv Z. Trehalose promotes Rhodococcus sp. strain YYL colonization in activated sludge under tetrahydrofuran (THF) stress. Front Microbiol [Internet] 2015 May 13. https://doi.org/10.3389/fmicb.2015.00438/abstract [cited 2023 Apr 18];6. Available from:.

[27] Jo Y, Rhee C, Choi H, Shin J, Shin SG, Lee C. Long-term effectiveness of bioaugmentation with rumen culture in continuous anaerobic digestion of food and vegetable wastes under feed composition fluctuations. Bioresour Technol 2021 Oct; 338:125500.

[28] Hua B, Cai Y, Cui Z, Wang X. Bioaugmentation with methanogens cultured in a micro-aerobic microbial community for overloaded anaerobic digestion recovery. Anaerobe. 2022 Aug;76:102603.

[29] Tsapekos P, Kougias PG, Treu L, Campanaro S, Angelidaki I. Process performance and comparative metagenomic analysis during co-digestion of manure and lignocellulosic biomass for biogas production. Appl Energy 2017 Jan;185:126–35.

[30] APHA, WEF. Standard methods for the examination of water and wastewater. In: American Public Health Association [Internet] 2005; 2005. Available from: https://www.apha.org/.

[31] Biosense Solutions [Internet]. Available from: https://biosensesolutions.dk/general-microbiology/; 2017.

[32] Altschul SF, Gish W, Miller W, Myers EW, Lipman DJ. Basic local alignment search tool. J Mol Biol 1990 Oct;215(3):403–10.

[33] Sievers F, Higgins DG. Clustal Omega. Curr Protoc Bioinforma [Internet] 2014 Dec; 48(1). https://doi.org/10.1002/0471250953.bi0313s48 [cited 2023 Apr 18]; Available from.

[34] Ye J, Coulouris G, Zaretskaya I, Cutcutache I, Rozen S, Madden TL. Primer-BLAST: a tool to design target-specific primers for polymerase chain reaction. BMC Bioinform 2012 Dec;13(1):134.

[35] Brankatschk R, Bodenhausen N, Zeyer J, Bürgmann H. Simple absolute quantification method correcting for quantitative PCR efficiency variations for microbial community samples. Appl Environ Microbiol 2012 Jun 15;78(12): 4481–9.

[36] Peirson SN. Experimental validation of novel and conventional approaches to quantitative real-time PCR data analysis. Nucleic Acids Res 2003 Jul 15;31(14): 73e–73.

[37] Aguilar-Moreno GS, Navarro-Cerón E, Velázquez-Hernández A, Hernández-Eugenio G, Aguilar-Méndez MÁ, Espinosa-Solares T. Enhancing methane yield of chicken litter in anaerobic digestion using magnetite nanoparticles. Renew Energy 2020 Mar;147:204–13.

[38] Yang Z, Wang W, Liu C, Zhang R, Liu G. Mitigation of ammonia inhibition through bioaugmentation with different microorganisms during anaerobic digestion: selection of strains and reactor performance evaluation. Water Res 2019 May;155: 214–24.

[39] Anderson KL, Apolinario EE, Sowers KR. Desiccation as a long-term survival mechanism for the archaeon *Methanosarcina barkeri*. Appl Environ Microbiol 2012 Mar;78(5):1473–9.

[40] Duan H, He P, Zhang H, Shao L, Lü F. Metabolic regulation of mesophilic *Methanosarcina barkeri* to ammonium inhibition. Environ Sci Technol 2022 Jun 21; 56(12):8897–907.

[41] Chang Bejarano A, Champagne P. Optimization of biogas production during start-up with electrode-assisted anaerobic digestion. Chemosphere. 2022 Sep;302: 134739.

[42] Vargas M, Malvankar NS, Tremblay PL, Leang C, Smith JA, Patel P, et al. Aromatic amino acids required for pili conductivity and long-range extracellular electron transport in *Geobacter sulfurreducens*. Giovannoni SJ, editor. mBio 2013 May;4(2). e00105-13.

[43] Liu X, DJF Walker, Nonnenmann SS, Sun D, Lovley DR. Direct observation of electrically conductive pili emanating from *Geobacter sulfurreducens*. Papoutsakis ET, editor. mBio [Internet] 2021 Aug 31;12(4). https://doi.org/10.1128/mBio.02209-21 [cited 2022 Feb 28]; Available from:.

[44] Reguera G, McCarthy KD, Mehta T, Nicoll JS, Tuominen MT, Lovley DR. Extracellular electron transfer via microbial nanowires. Nature. 2005 Jun;435 (7045):1098–101.
[45] Pielberg G, Day AE, Plastow GS, Andersson L. A sensitive method for detecting variation in copy numbers of duplicated genes. Genome Res 2003 Sep;13(9): 2171–7.
[46] Murphy CL, Yang R, Decker T, Cavalliere C, Andreev V, Bircher N, et al. Genomes of novel *Myxococcota* reveal severely curtailed machineries for predation and cellular differentiation. Nikel PI, editor. Appl Environ Microbiol 2021 Nov 10;87 (23). e01706-21.